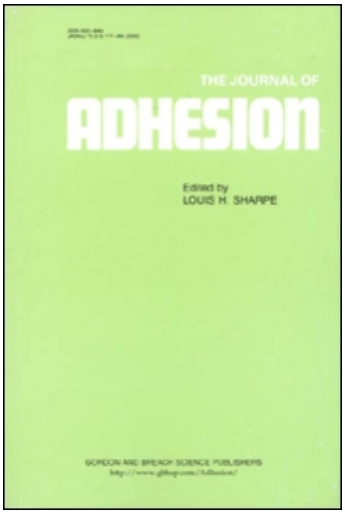

The Journal of Adhesion

Publication details, including instructions for authors and subscription information:
http://www.informaworld.com/smpp/title~content=t713453635

On the Uniformity of Stresses in Some Adhesive Deformation Specimens

K. M. Liechti[a]; T. Hayashi[a]
[a] Department of Aerospace Engineering and Engineering Mechanics, The University of Texas at Austin, Austin, TX, U.S.A.

To cite this Article Liechti, K. M. and Hayashi, T.(1989) 'On the Uniformity of Stresses in Some Adhesive Deformation Specimens', The Journal of Adhesion, 29: 1, 167 — 191
To link to this Article: DOI: 10.1080/00218468908026486
URL: http://dx.doi.org/10.1080/00218468908026486

J. Adhesion, 1989, Vol. 29, pp. 167–191
Reprints available directly from the publisher
Photocopying permitted by license only

Printed in the United Kingdom

On the Uniformity of Stresses in Some Adhesive Deformation Specimens†

K. M. LIECHTI and T. HAYASHI

Department of Aerospace Engineering and Engineering Mechanics, The University of Texas at Austin, Austin, TX 78712, U.S.A.

(Received August 19, 1988; in final form November 9, 1988)

The stress distributions within napkin-ring, cone-and-plate and stiff-adherend specimens were determined under shear, bond-normal and thermal loadings using linear elastic finite element analysis. Modifications to adherend edges were also considered in order to improve uniformity. The stiff-adherend specimen showed the most promise for use as a specimen for determining the deformation behavior of adhesives *in-situ*. A stiff-adherend specimen having rounded adherends provided the most uniform stress state, free from any stress concentrations, a result that was qualitatively confirmed in experiments.

KEY WORDS Adhesive stress-strain behavior; napkin-ring specimen; cone-and-plate specimen; stiff-adherend specimen; finite element stress analysis; stress concentrations.

INTRODUCTION

Perhaps the greatest amount of feedback on the development of new adhesives and surface preparations has been provided by single lap shear testing. The single lap shear specimen is very easy to prepare and test and the lap shear strength, the maximum load divided by the bond area, is taken to be the strength of the adhesive. At the same time it has long been recognised[1,2] that the lack of complete tensile and bending rigidity in the adherends leads to differential shear and bending in the joint that in turn produces nonuniform shear stresses and introduces peeling stresses in the adhesive layer. Even if the adherends were absolutely rigid, a nonuniform shear stress would still arise due to the stress concentrations that occur at the bimaterial corner[3] formed by the adhesive termination and the adherend. Thus, while the single lap shear specimen appears to be useful for ranking adhesive formulations, novel surface preparations and the severity of various environments, the lap shear strengths are not really the strength of the adhesive and cannot be used as a design parameter. A further

† Presented at the 35th Sagamore Army Materials Research Conference, Manchester, New Hampshire, U.S.A., June 26–30, 1988.

consideration is that the stiffness of the adhesive and any plastic, viscoelastic response, etc. must also be known for rational joint design. Thus the displacements as well as the stress state must be measured in any specimen that is being used to determine adhesive constitutive behavior. Although the elastoplastic behavior of various adhesives determined from neat resin tests has been used to explain differences in the load deflection response of a single lap shear specimen,[4] thus suggesting an inverse approach to the determination of adhesive constitutive behavior, the approach being considered here has been to find specimens that provide a high degree of uniformity and purity of stress states within the adhesive. Some of the attempts to obtain more uniform stress states have been based on modifications to the single lap shear specimen. The double lap shear specimen reduces the severity of bending deformations by its more symmetric arrangement. Nonetheless, peeling and bimaterial corners still give rise to impure and nonuniform stress states.[5] Another possibility is the thick adherend single lap shear specimen first suggested by Frazier[6] for fatigue testing of structural adhesives. However, a very thorough examination by Guess *et al.*[7] found that although the thick adherends greatly reduced peeling, there were still concentrations towards the adhesive edges. Continuing the family of tensional shear specimens, Arcan has recently proposed the stiff-adherend specimen[8] based on specimen geometry that had been earlier developed for pure shear testing of homogeneous[9] and composite materials.[10] In comparing adhesive shear stresses in the stiff-adherend specimen and the thick-adherend single lap joint, it was found that shear stress concentrations were reduced by one third in the stiff-adherend specimen.

The other approach to shear testing is to apply torsional loads. The most commonly used configuration in this regard is the napkin-ring specimen[11] which gives rise to a reasonably uniform shear stress if the ratio of the wall thickness to the diameter is kept small. The cone-and-plate specimen, commonly used for viscous fluids, has recently been proposed as an alternative torsional shear specimen.[12] Based on the assumption that the adherends were rigid, it was shown that the shear stress distribution was more uniform than that of the napkin ring. For the structural adhesives that are being considered, the rigidity assumption is not valid[13,14] and the consequences will be further considered here.

The purpose of the work presented here is to compare the stress distributions in the napkin-ring, cone-and-plate and the stiff-adherend specimens under shear, bond-normal and thermal loads. The motivation for the shear load is obvious. The bond-normal loading was considered because slight misalignments might induce such displacements across the adherends. Another reason is that, as adhesive joint analyses become more sophisticated, they will have to account for multiaxial yielding of adhesives, and there will be a need for specimens that provide uniform stresses under bond-normal loading so as to establish multiaxial yield criteria. The thermal loading considered here is due to cooldown following cure. The residual stress state is likely to be quite severe for the 371°C (700°F) structural adhesives that are currently being developed.

When tensional shear, bond-normal and thermal loadings are considered, the

possibility of stress concentrations at the bimaterial corners formed by adhesive terminations arises. If the adherends can be considered to be rigid, then the early work of Williams[15] on stress concentrations near angular corners provides some insight. For example, for clamped-free corners, it was found that no singularities arose for corners having angles less than 60°. More general singularity analyses have been conducted by Hein and Erdogan[3] who considered a range of relative stiffnesses in the bimaterials having Poisson ratios of 0.2, but still found that if the wedge angle of the stiffer component is less than about 60°, then no singularities arise. The effect of Poisson's ratio is quite strong and the 60° angle reduces to 45° for incompressible materials.[16] Accordingly, various local modifications to the adherends such as rounding and bevelling adherend edges have been considered in order to improve the uniformity of stresses in the adhesive layer of the specimens considered. Shear tests were conducted on the most promising specimen identified by stress analyses and qualitatively confirmed the purity and uniformity of the stress state.

STRESS ANALYSIS

The stress analysis of the specimens was conducted using the finite element codes VISTA[17] and TEXPAC-NL[18] (for torsional loadings). The adherends and adhesive were taken to be isotropic, linearly elastic materials. The adherends were considered to be aluminum with Young's modulus, Poisson's ratio and coefficient of thermal expansion of 68.95 GPa, 0.33 and 18×10^{-6} mm/mm/°C, respectively. The corresponding adhesive properties were 2.32 GPa, 0.4 and 54×10^{-6} mm/mm/°C. Shear, bond-normal and thermal loadings were applied to each specimen. The shear loading was applied either by a torque or by a tension-shear load. The bond-normal loading was usually provided by applying a displacement of 25.4 μm normal to the bondline. The thermal loading was due to a cooldown to 21°C from a (stress free) cure temperature of 121°C. Initially, there were at least four layers of elements through the adhesive thickness with similar lengthwise meshing near adhesive terminations. As the most promising geometries were identified, the degree of refinement near edges was increased so that element lengths were on the order of 0.01 mm near corners. Each stress distribution was usually normalized by dividing the local stress by an average normal or shear stress, σ_0 or τ_0 respectively. In view of the mesh refinements near the edges, a weighted average was taken whose form was

$$\sigma_0 = \sum_{n=2}^{m} \frac{(\sigma_n + \sigma_{n-1})}{2} \frac{(x_n - x_{n-1})}{L} \tag{1}$$

where m = number of points at which the stress was evaluated
x = location along the bondline
L = length of the bondline

In order to summarize the results later, a "uniformity coefficient" was defined as the fraction of the length of the bondline over which the stresses were within $\pm 10\%$ of σ_0 or τ_0.

The stress distributions in the specimen families based on the napkin-ring, cone-and-plate and stiff-adherend specimen are now presented. From the initial results, various modifications were considered in order to try to improve uniformity.

Napkin ring

The basic napkin-ring geometry that was considered is shown in Figure 1a and essentially consists of two adherend tubes butt-joined by a ring of adhesive material. Under a torque T, the shear stress, τ, at some location, r, can be obtained from

$$\tau = \frac{2Tr}{\pi(R_o^4 - R_i^4)} \tag{2}$$

According to this equation and dimensions noted in Figure 1a, the shear stress is within 3% of the mean value throughout the adhesive layer, a very uniform distribution. However, when subjected to bond-normal displacements over the top surface of the upper adherend, there are significant stress concentrations (Figure 2) near the adhesive edges corresponding to the inner and outer radii. Furthermore, the stresses in the interior are nonuniform due to the constraint

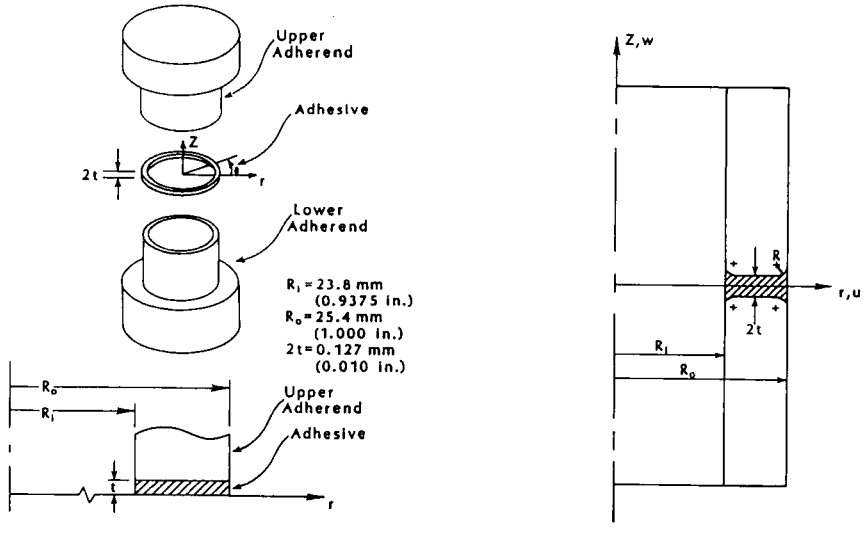

a) Flat Adherends b) Rounded Adherends

FIGURE 1 Napkin ring specimen geometries.

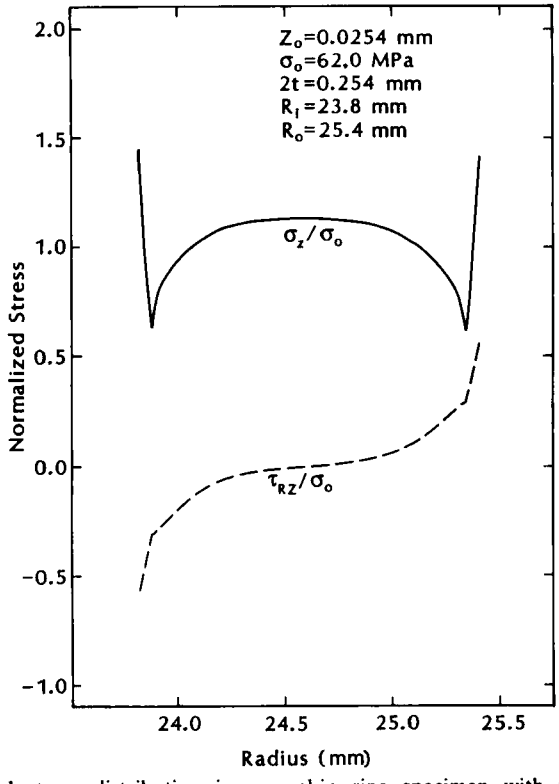

FIGURE 2 Normal stress distribution in a napkin ring specimen with flat adherends under bond-normal loading.

applied by the adherends.[19] The uniformity coefficient was only 75%, and thermal loading was therefore not considered.

The stress concentrations noted above are due to the sharp bimaterial corners produced by the adhesive and adherend. In view of the findings of Williams and Hein and Erdogan discussed earlier, consideration was given to rounding the adherend edges as indicated in Figure 1b. Various rounding radii were evaluated,[20] and it was found that rounding the adherend edges to a radius that was equal to the adhesive layer thickness, $2t$, eliminated the edge stress concentrations in axial stress when the joint was loaded normal to the bondline (Figure 3b). However, the rounding slightly disturbed the uniformity of the shear stress produced by a torsional loading (Figure 3a) and did not eliminate stress concentrations in the residual stresses (Figure 3c). Adams and Coppendale,[21] in considering the effect of adhesive spew fillets, also found that stress concentrations could be induced under shear loading. Various bevelled adherend geometries were also considered,[20] but the resulting stress distributions were all less uniform than those produced by rounding. Thus, while the napkin ring specimen produces highly uniform shear stresses under torsional loading, and rounding of

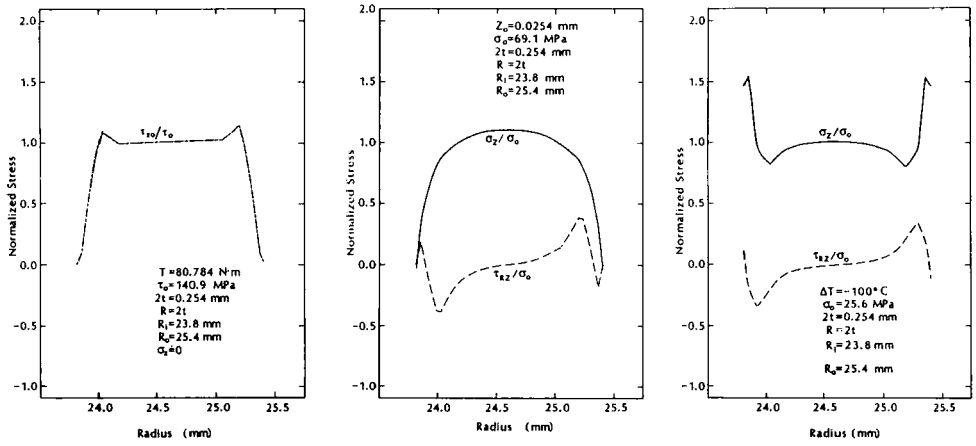

a) Shear b) Bond-Normal c) Thermal

FIGURE 3 Stresses in a napkin ring specimen with rounded adherends under shear, bond-normal and thermal loadings.

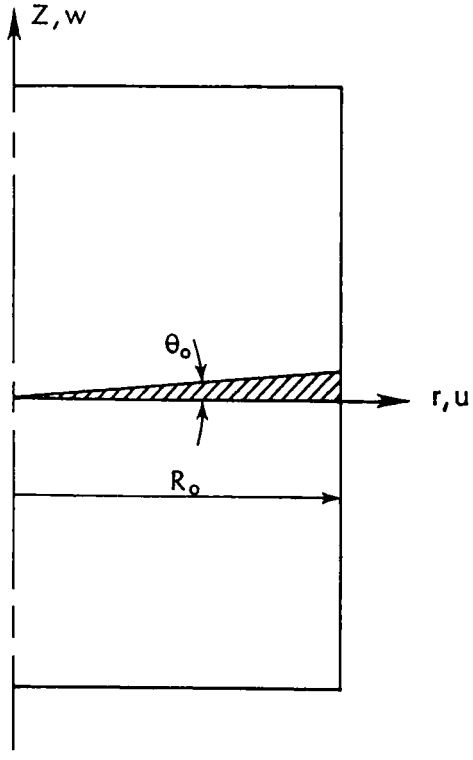

FIGURE 4 Cone-and-plate specimen geometry.

the adherends eliminated stress concentrations under bond-normal loading, the residual stress state was always singular for the modifications that were considered.

Cone-and-plate specimen

The cone-and-plate specimen geometry is shown in Figure 4 and consists of solid circular lower and upper adherends having flat and conical surfaces, respectively, to define the adhesive volume. The outer radius R_o was taken to be 12.7 mm, and the cone angle θ_0 was 3°. Using the typical properties of an aluminum/epoxy specimen we can see (Figure 5a) that the shear stress produced by shear loading is higly nonuniform in the radial direction, although there is not much variation through the thickness. The essentially constant shear stress produced by rigid adherends[12] is only approached for the steel/rubber combination[14,20] where the modulus ratio was 6×10^4. The nonuniform shear stress is accompanied by high

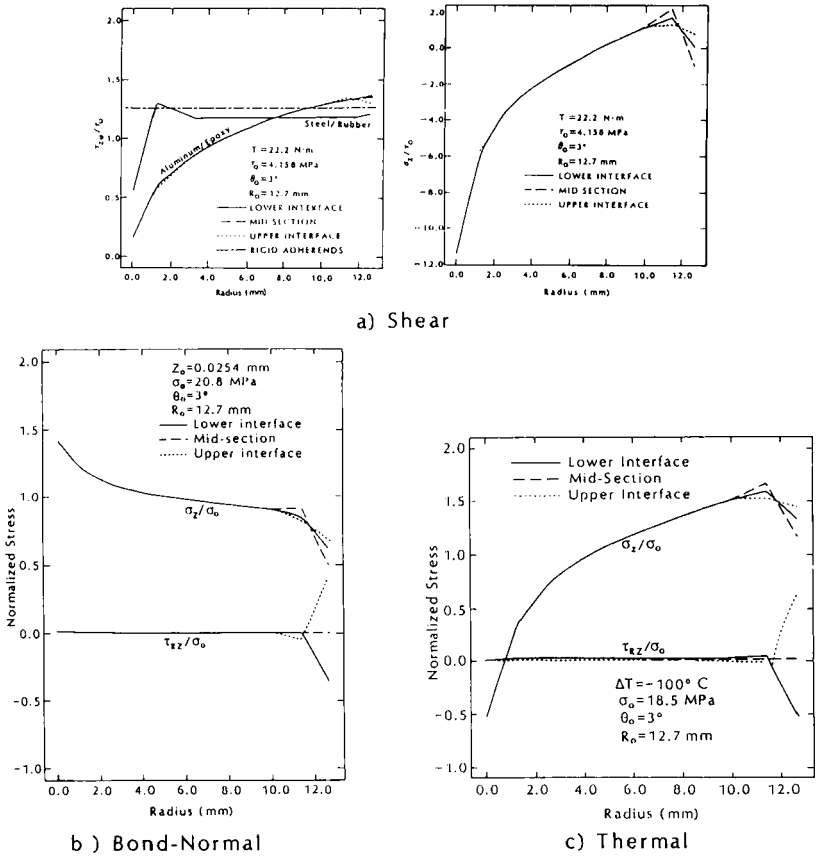

FIGURE 5 Stresses in a cone-and-plate specimen subjected to shear, bond-normal and thermal loadings.

compressive axial stresses towards the specimen center. The situation is somewhat improved under bond-normal loading (Figure 5b) where the axial stress is more uniform than that generated by the shear loading and the thermal loading (Figure 5c).

The modification that was considered here was to drill a central hole along the axis of the specimen so that it became hollow. It can be seen from Figure 6 that the removal of the central material is quite beneficial for the shear and bond-normal loadings. Under the former, the shear stress has become much more uniform although the nonuniform compressive axial stresses are still very evident. The residual stresses (Figure 6c) were relatively unaffected by the hole drilling. The uniformity coefficients were 50%, 73% and 27% for the shear, bond-normal and thermal loads, respectively, making the specimen generally undesirable for use with structural adhesives.

Stiff-adherend specimen

The final set of specimens that was considered was the stiff-adherend specimen,[8] a modification of a specimen that was employed for the shear testing of homogeneous materials. The specimens are attached (Figure 7) to the S-shaped grips in the central region, and a tensile load applied to the grips parallel to the bondline produces shear in the adhesive. Based on the experience with the napkin-ring specimen, various bond terminations were considered. The basic specimen geometry, straight notch with sharp adherends (SNSA), is shown on the left in Figure 7b. The first modification was to round the adherends in the same way that the napkin ring adherends were rounded ($R = 2t$). The configuration was called straight notch with rounded adherends (SNRA) and is the central specimen in Figure 7b. Another possibility was the rounded notch with sharp adherends (RNSA), shown to the right in Figure 7b. The overall specimen geometries differ

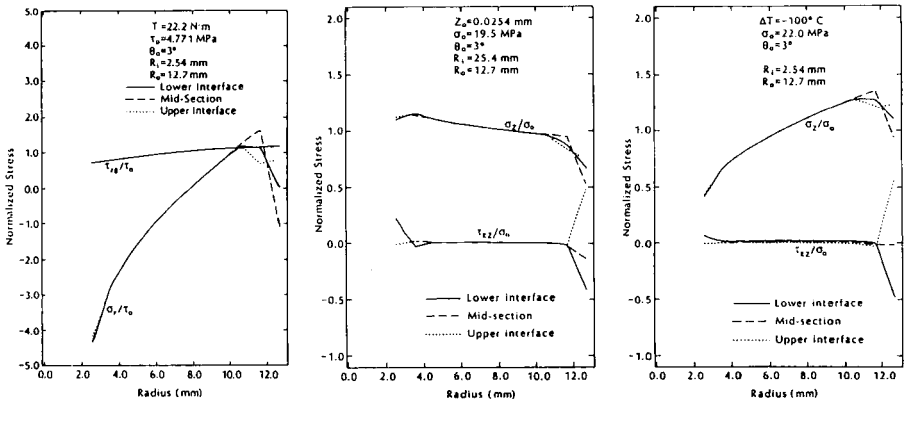

a) Shear b) Bond-Normal c) Thermal

FIGURE 6 Stresses in a cone-and-plate specimen with a central hole subjected to shear, bond-normal and thermal loadings.

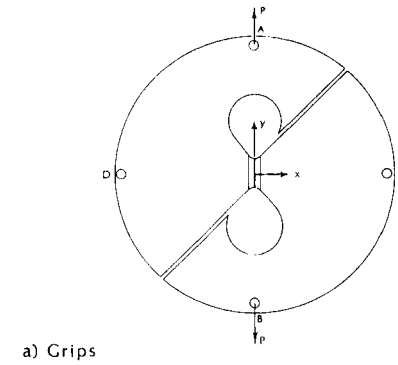

a) Grips

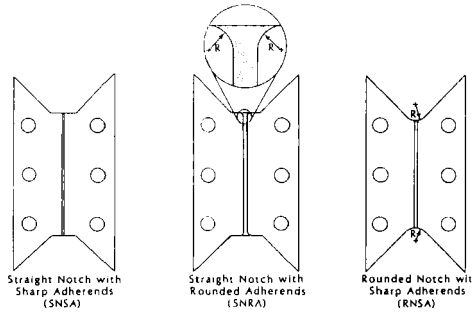

b) Specimens

FIGURE 7 Stiff-adherend specimens and grips.

from that proposed in Ref. 8 because this work was underway prior to and independent of the publication of Ref. 8. The longer bond length (50.8 mm) is due to a desire to obtain uniform stresses under bond-normal loading which in turn requires a large aspect ratio (bond length to bond thickness) in order to minimize the "poker chip" effect.[19]

The interfacial stress distributions in the three specimen geometries under shear loading are shown in Figure 8 in standard and semilogarithmic form. For all stiff adherend results, the normalizing stress was the load divided by the area. The ζ parameter is the distance from the specimen edge normalized by the adhesive thickness and was plotted logarithmically to bring out the details of the stress distribution. The high degree of refinement for the SNRA and RNSA was obtained by rezoning. In this procedure, a region of interest is defined and further subdivided into smaller elements, the boundary conditions for the refined region being provided by the solution obtained from the coarse mesh analysis. Under the shear loading $P = 13.8$ kN at point A, reacted at B, Figure 7, it can be seen that the shear stress in all three specimen geometries is reasonably uniform. The uniformity coefficient in shear stress was 80, 80 and 96% for the SNSA, SNRA, RNSA, respectively. Although the rounded notch increased the uniformity of

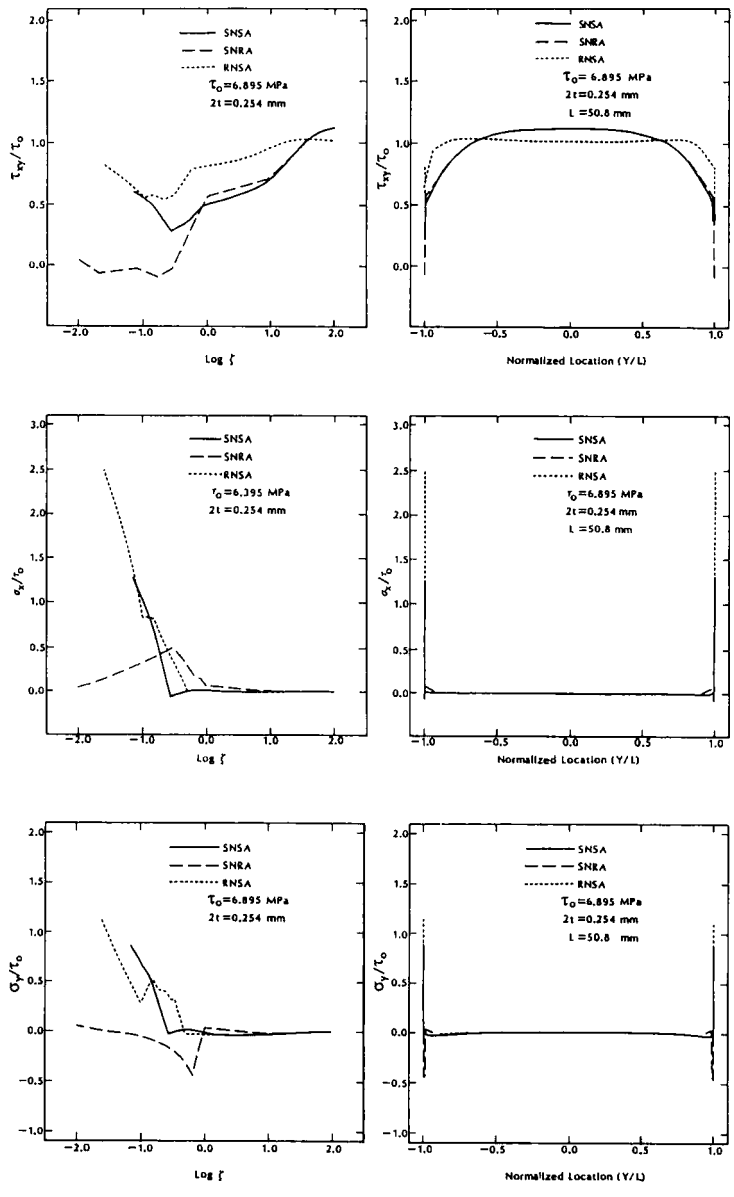

FIGURE 8 Stresses in stiff-adherend specimens under shear loading.

stresses, the semilogarithmic plots indicate sharp rises in both interfacial stresses near the edge. The stress-free condition on the edge requires that τ_{xy} must return to zero but σ_x may be singular. On the other hand, rounding the adherends to a radius equal to the adhesive layer thickness eliminated the increases in both interfacial stress components very close to the specimen edge.

To analyze the response to a bond-normal loading, a load $P = 13.8\,\text{kN}$ was

applied at the point C, while point D (Figure 7) was fixed. Again (Figure 9) the rounded notch (RNSA) gave the highest degree of uniformity (91%) in bond-normal stress, σ_x, while the straight notch with rounded adherend (SNRA) gave rise to a lesser degree of uniformity (82%) but no stress concentrations.

The residual stress distributions (Figure 10) were only determined for the SNSA and SNRA specimens because it was felt that the RNSA specimen could be notched after cure, making sure to remove enough material to eliminate stress

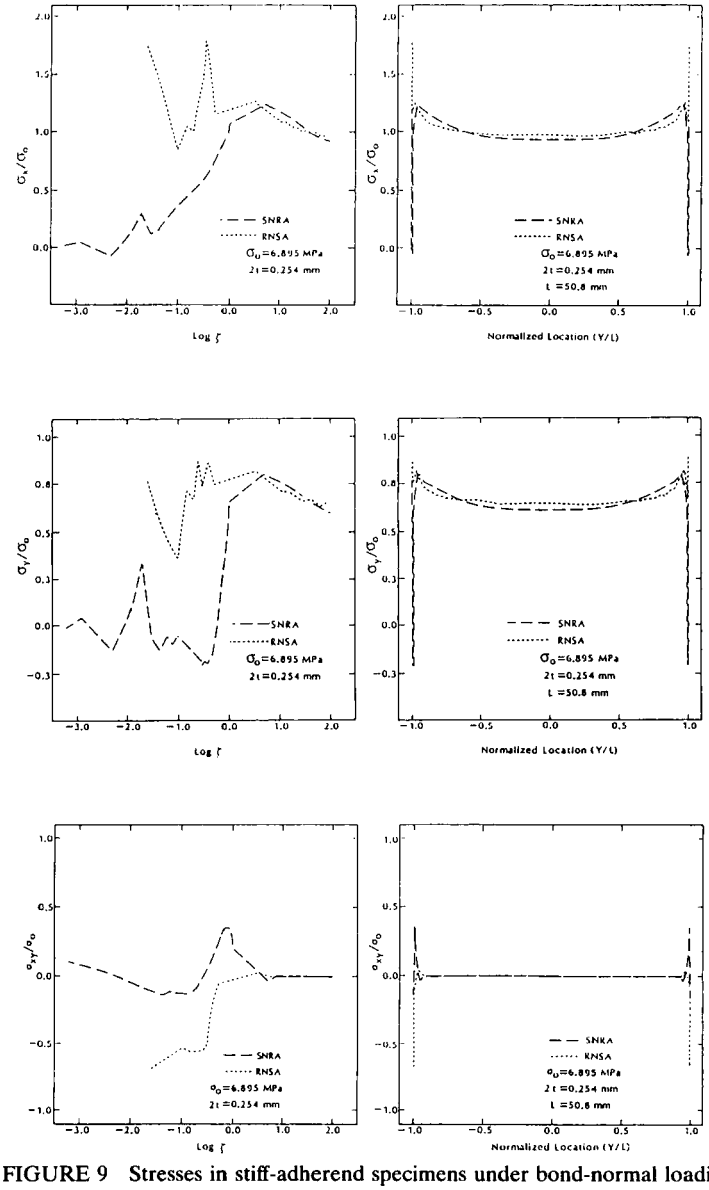

FIGURE 9 Stresses in stiff-adherend specimens under bond-normal loading.

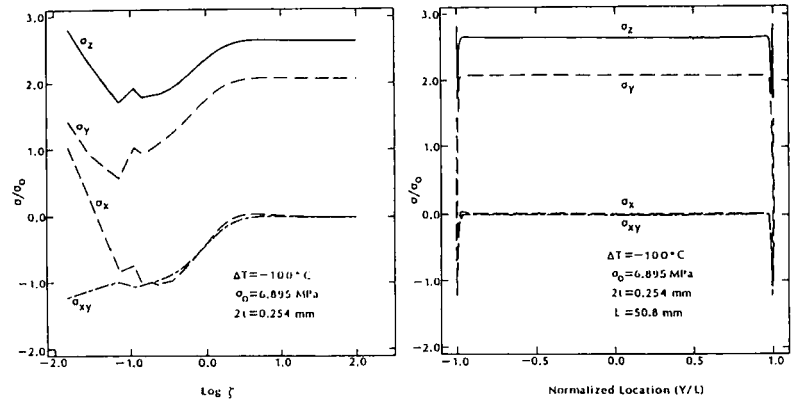

a) Straight Notch with Sharp Adherends (SNSA)

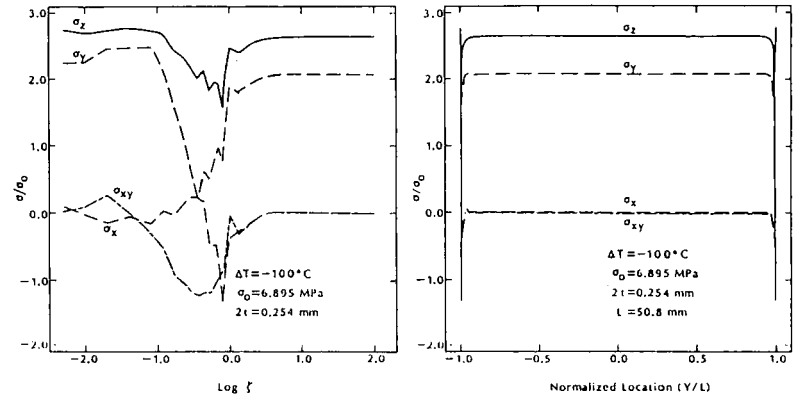

b) Straight Notch with Rounded Adherends (SNRA)

FIGURE 10 Residual stresses in stiff-adherend specimens.

concentrations entirely. In both geometries the shear and bond-normal residual stresses were mostly zero and therefore do not contribute to the dominant stresses in shear and bond-normal loading. The SNSA showed an increase in all stresses as the bond edge was approached while maintaining uniformity of stresses over 98% of the bond length. Rounding the adherends (SNRA) caused a dip in the stresses about one bond thickness in from the edge, but they rose and became constant closer to the bond edge with no signs of singular behavior. The uniformity coefficient increased to 99% and with such high uniformity coefficients the feasibility of fabricating RNSA specimens from SNSA specimens with no residual stress concentration is clearly established. Nonetheless, the nonzero components are between two and three times the average bond-normal stress produced by a bond-normal loading of 13.8 kN and could be as high as the failure

stress for the 350°C cooldown envisaged for high temperature adhesives. Among the stiff-adherend specimens, the straight notch with rounded adherends (SNRA) is preferable because if did not give rise to any stress concentrations under any of the loadings, even though the RNSA produced a higher uniformity coefficient.

In order to summarize the results from all of the geometries that were analyzed, the uniformity coefficients for each case were compared in the bar graph depicted in Figure 11. The percentages are grouped together for each type of loading. As mentioned previously, the uniformity coefficients were usually sacrificed in an attempt to reduce stress concentrations near bimaterial corners. Therefore, the most promising specimen was not only determined by highest uniformity coefficient; the degree of stress concentration also played a strong role in the selection. Thus, for example, within the modified napkin ring family, the flat adherends had the greatest uniformity coefficient under bond-normal and

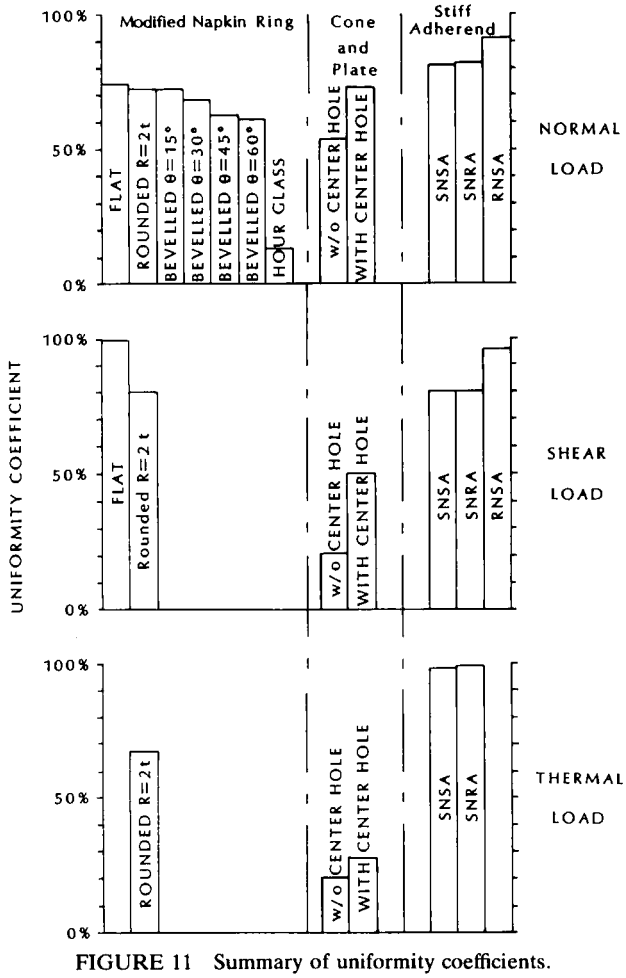

FIGURE 11 Summary of uniformity coefficients.

shear loads. However, there were no stress concentrations in the specimens with rounded adherends and so even though its uniformity coefficient was less, it was judged to be the more desirable specimen. In comparing uniformity coefficients from family to family, the cone-and-plate values were generally the lowest. Under shear loads, the napkin-ring specimen with flat adherends had the greatest degree of uniformity, followed by the stiff-adherend specimen with the rounded notch and sharp adherend. The rounded adherend napkin-ring and other modified stiff-adherend geometries came next with roughly the same degree of uniformity. However, the stiff-adherend geometries consistently outperformed all other geometries under bond-normal and thermal loads. Of the stiff-adherend geometries, the rounded notch with sharp adherends (RNSA) provided the greatest degree of uniformity under all loadings. However, the sharp adherends gave rise to stress concentrations. The geometry with straight notch with rounded adherends (SNRA) was therefore judged to be the most desirable geometry overall because it gave rise to a reasonable uniformity coefficient without stress concentration. The procedures for fabricating and testing the specimen are now described.

TEST PROCEDURES AND RESULTS

The detailed geometry of the SNRA specimen and associated grips that was tested here is shown in Figure 12. The bond line length was chosen to be 50.8 mm in order to ensure uniformity under bond-normal loading,[19] and the remaining dimensions were determined proportionally from ratios given by Arcan *et al.*[10] The outer outer radius of the grips was therefore 190.5 mm which is large but could be reduced substantially if only shear testing was evisaged.[8,13] The grips were made of stainless steel and the specimen had aluminum adherends bonded with FM 300, a modified epoxy adhesive film supported by a polyester carrier.† In order to obtain a number of specimens having the same processing history, blocks of aluminum having the same planform geometry shown in Figure 12 were bonded together (Figure 13). Two blocks were machined to other dimensions shown in Figure 13, the 76.2 mm length being chosen to yield approximately ten specimens having 6.34 mm thickness. Once the blocks were made, the edges having the 76.2 mm length were rounded to a radius of 0.254 mm which was checked under the microscope. After cleaning the adherend blocks with soap and water, the bonding surfaces were scrubbed with an industrial cleanser and abrasive pad, rinsed with tap water, etched in sodium dichromate/sulfuric acid for 20–30 minutes, rinsed with distilled water, oven dried at 55–64°C for 15–20 minutes, sprayed with BR127† primer to dry thickness of 2.5 to 5.0 μm, air dried for 30 minutes and finally oven dried for 30 minutes at 121°C. The adhesive tape was vacuum dried prior to application to the adherend blocks, and bond

† Product of American Cyanamid whose furnishing of material is gratefully acknowledged.

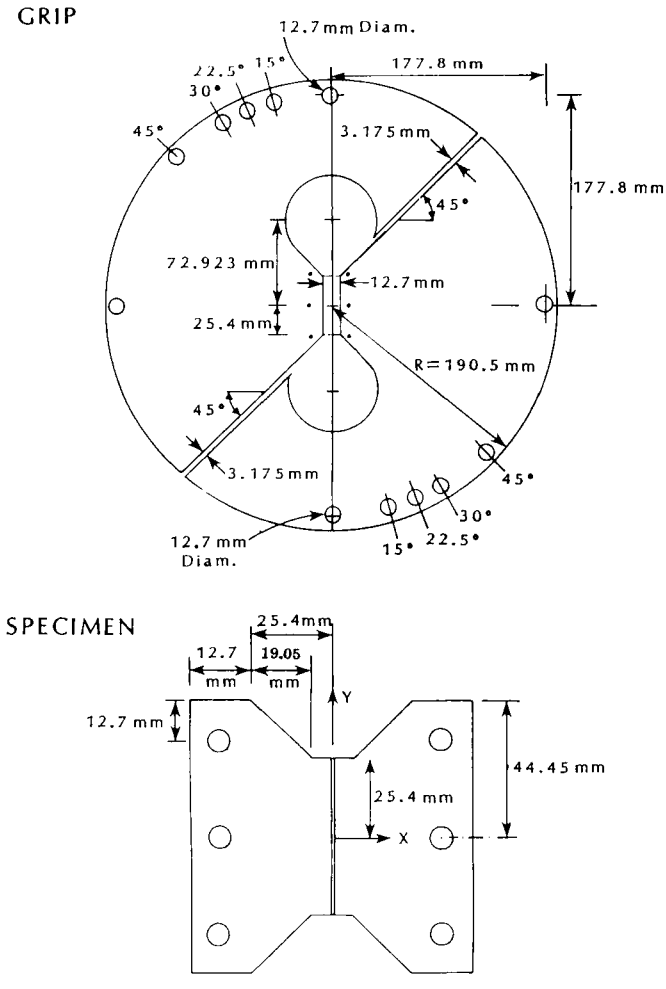

FIGURE 12 Dimensions of the stiff-adhered specimen and grips.

thickness was maintained by metal shims at 0.254 mm ± 0.0508 mm. The assembly was placed in a preheated press and allowed to stabilize at 121°C. A pressure of 100 KPa to 340 Kpa was slowly applied while the temperature was raised to 175°C in 30 minutes in order to bring out air bubbles. Cure was completed at 175°C for 60 minutes with a slow cool to room temperature. The 6.35 mm thick specimens were then sliced from the bonded block using a circular cutter. The circular cut was followed by a milling step with a fly-cutter so that the surfaces could be polished to facilitate microscopic observation of the bondline during testing. The latter steps would not be necessary in a production environment.

The first step in the testing was to align the grips properly with the loading axis. The yokes that connected the grips to the uniaxial, servohydraulic loading device had two pairs of holes so that each grip could be fixed independently. With the

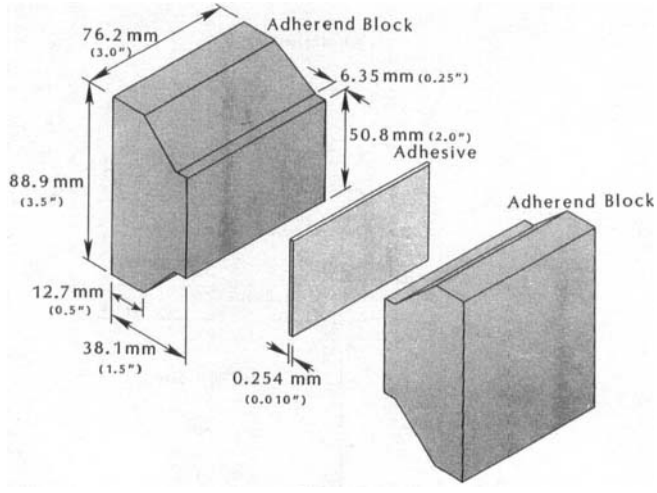

FIGURE 13 Schematic view of specimen assembly.

grips aligned, a blank specimen (no bolt holes) was inserted into the grip slots and a microvideo system, consisting of a microscope, video camera, recorder, analyzer and monitor (Figure 14a) was used to make sure that the bond line was parallel to the load axis. Once the specimen was satisfactorily aligned, a transfer punch was used to mark the centers of the six holes in the grips onto the specimen. The specimen was the removed so that the holes could be drilled.

In the original gripping procedure, after the holes had been drilled, the specimen was reinserted into the grip slots and was secured by bolts so that the specimen boundaries were essentially clamped. As will be noted later in the results section, slippage between the grips and the specimen usually occurred at some point during the loading, no matter how much clamping force was applied. As an alternative, the bolts were replaced by pins so that the loads were transferred from the grips to specimen by bearing on the pins rather than clamping. There were no signs of slippage with this procedure. The specimen was apparently able to "settle" into a stable configuration more easily.

The shear strain was measured using the extensometer shown in Figure 14b. Although the extensometer is usually used for measurements of longitudinal and transverse strain in uniaxial tension specimens, it was adapted for the present purposes using only one longitudinal channel. Left and right extensometer bases were clamped to the left and right adherends very close to the adherend/adhesive interface. The two upper legs and the lower right-hand leg of the transducer were attached to an adapter mounted to the right-hand base. The lower left-hand leg of the extensometer was attached to a second adaptor that was mounted to the left-hand base. A relative longitudinal motion of one adherend with respect to the other therefore resulted in a relative movement between the left upper and lower legs of the extensometer, exciting a signal from the strain gage placed on the lower leg of the extensometer. The extensometer was calibrated at 0.254 mm/volt and the resolution in relative shear motion of the adherends was taken to be

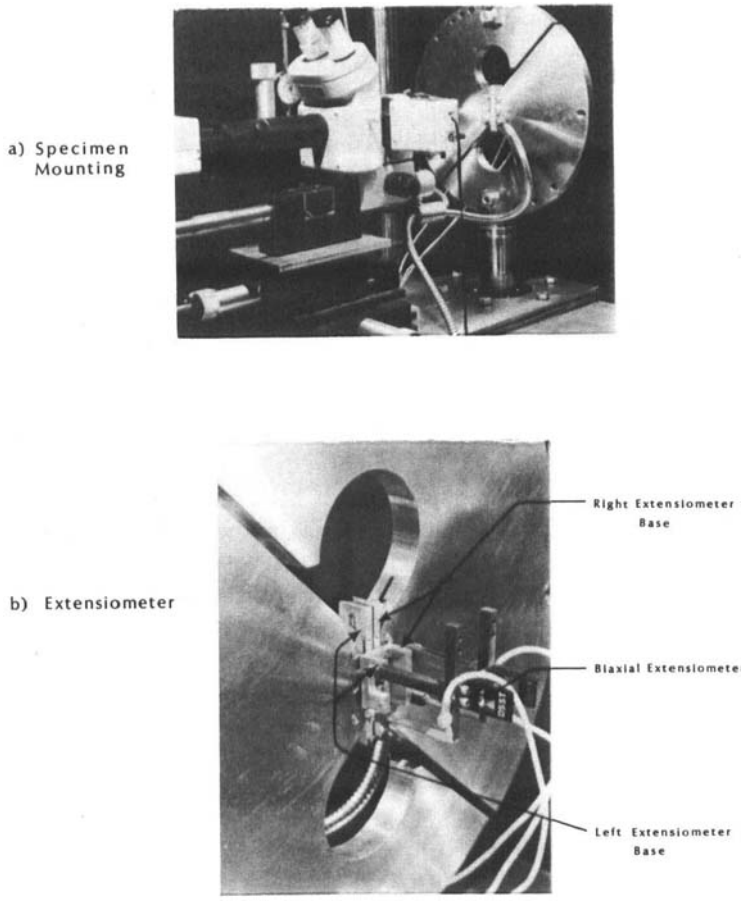

FIGURE 14 Specimen and extensometer mounting.

0.245 μm. The loads were measured using an 89 kN capacity load cell. The load and strain were recorded on a plotter during the tests which were conducted under displacement control at a rate of 33.87 μ7/sec.

RESULTS

Typical results are presented for the stress-strain behavior of FM 300. As indicated earlier, two methods of attaching the specimens to the grips were considered. Stress-strain curves are therefore presented for specimens that were clamped to the grips and specimens that were pinned to the grips. The shear stress in the adhesive was obtained by dividing the recorded loads by the shear cross-sectional area of the adhesive (50.4 mm $\times$ 6.35 mm). The shear strain was taken to be the displacement measured by the extensometer divided by the bond

line thickness. Any extension in the adherends between the extensometer bases and the adherend adhesive interface was, in effect, very small.

A typical shear stress-strain curve for a specimen that was clamped to the grips is shown in Figure 15. The data for the plot of small values of strain were obtained by suitable magnification of the extensometer signal and were to be used for determining the shear modulus. With the magnified mode, it can be seen that there is a sharp increase in slope for a strain of approximately 1.5%. The change in slope was associated with a lateral movement of the adherends as observed by the micro-video system. Once the lateral movement stopped, the slope of the stress-strain curve returned to an equal or slightly smaller value than was observed before lateral movement started. Furthermore, it was noticed that for specimens for which the load was manually decreased, following the return to initial slope, the unloading path showed no signs of deviation and the same was true for subsequent reloading. It was therefore concluded that some realignment had taken place. The shear modulus obtained from the initial tangent was 318 MPa. The ultimate shear strength was 32.86 MPa and the strain to failure was 42.2%. Following the attainment of the maximumum load, failure of the specimen seemed to take place in a gradual way, with microcracks opening up around scrim fibers as the load dropped. The fracture took place in the plane of the scrim cloth as can be seen (Figure 16) from the optical micrographs of the fracture surfaces. The top picture shows both fracture surfaces under low

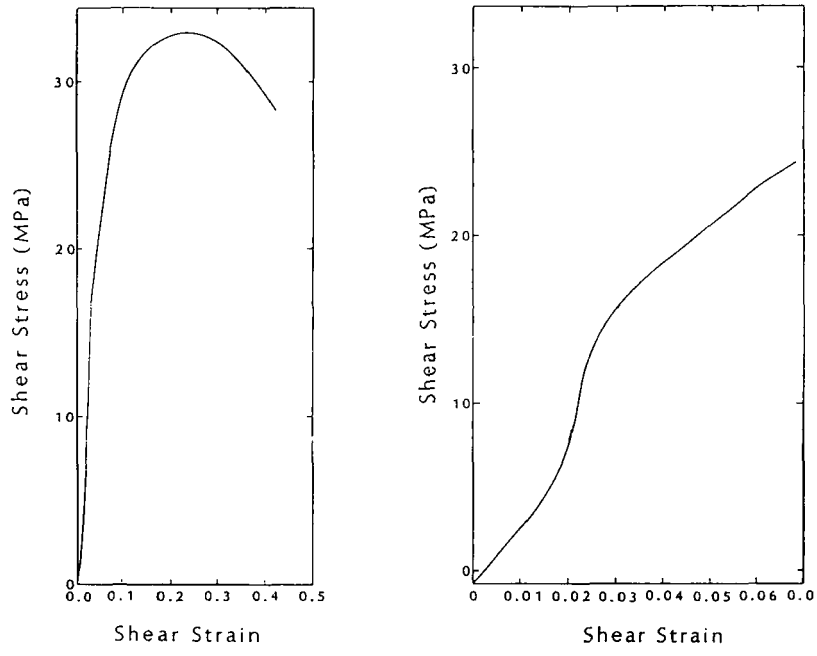

FIGURE 15 Shear stress-strain response of FM 300 tested under clamped boundary conditions.

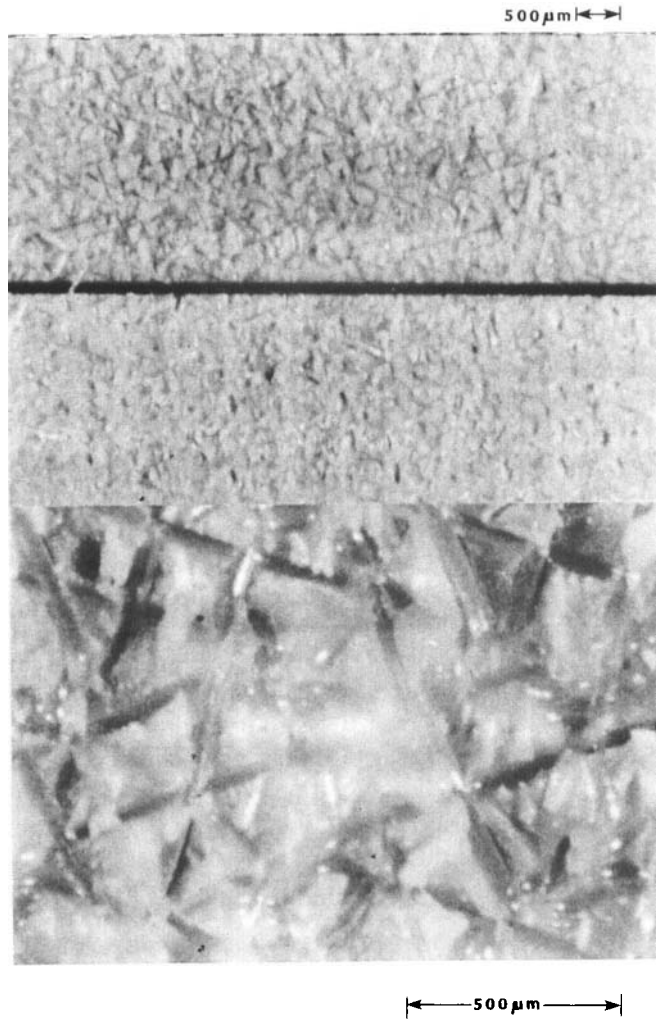

FIGURE 16 Fracture surfaces of a stiff-adherend specimen tested under clamped boundary conditions.

magnification, whereas the bottom is a close-up and shows the former locations of the scrim fibers that were embedded in the adhesive.

The overall stress-strain curve for FM 300 obtained from a specimen that was pinned to the grips is shown in Figure 17. In these cases there was no increase in the initial slope of the stress-strain curve in the magnified plots of strains up to 7%, as had been seen for the clamped case. Furthermore, no noticeable lateral movement of the adherends was observed in the micro-video system. The modulus derived from these data was found to be 347 MPa. The ultimate shear strength was 45 MPa with a strain to failure of 41%. The fracture surface from the pinned specimen was quite different from those observed in specimens that had

been tested under clamped conditions. They were much rougher (Figure 18), having very regular ridges running perpendicular to the load direction. Scrim fiber markings could be seen on some of the ridges. When the bond line was viewed in profile (Figure 19), it appears that the ridges were formed by microcracks that grew at 45° to the loading direction and then linked to cause final failure. The 45° orientation of the microcracks would imply that they grew perpendicular to the maximum principal stress direction. From the flatness of the stress-strain curve it appears that the microcrack growth was progressive in nature, but linkage did not occur until the failure strain approached. The microscopic observation with the video system also indicated that microcracks grew in a progressive manner, followed by a sudden parting of the specimen at the maximum strain.

Comparing the results from the two sets of data, it can be seen that the adhesive modulus differed by less than 10%. Since such variations can be encountered in tests conducted under similar conditions, it is unlikely that the noted difference can be attributed to gripping procedures. However, the ultimate strength of the adhesive that was tested under pinned conditions was 37% greater than the value obtained from specimens that had been clamped. The fracture surfaces were also quite different so that the shear strength was clearly affected by gripping procedure. The higher ultimate strength obtained under pinned conditions would suggest that pure shear was indeed attained because any bond-normal loading would reduce the strength in shear. The appearance of the fracture surfaces also suggests that pure shear was achieved under the pinned gripping conditions but not the clamped case. The rough ridges formed by microcracks aligned at 45° to the load axis suggest that pure shear existed when pinned gripping was used. The relatively flatter fracture surfaces that resulted from the clamped gripping indicate that tensile bond-normal stresses were also active. The

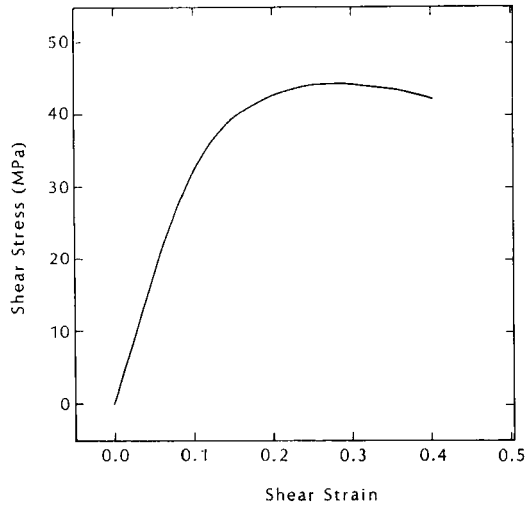

FIGURE 17 Shear stress-strain response of FM 300 tested under pinned boundary conditions.

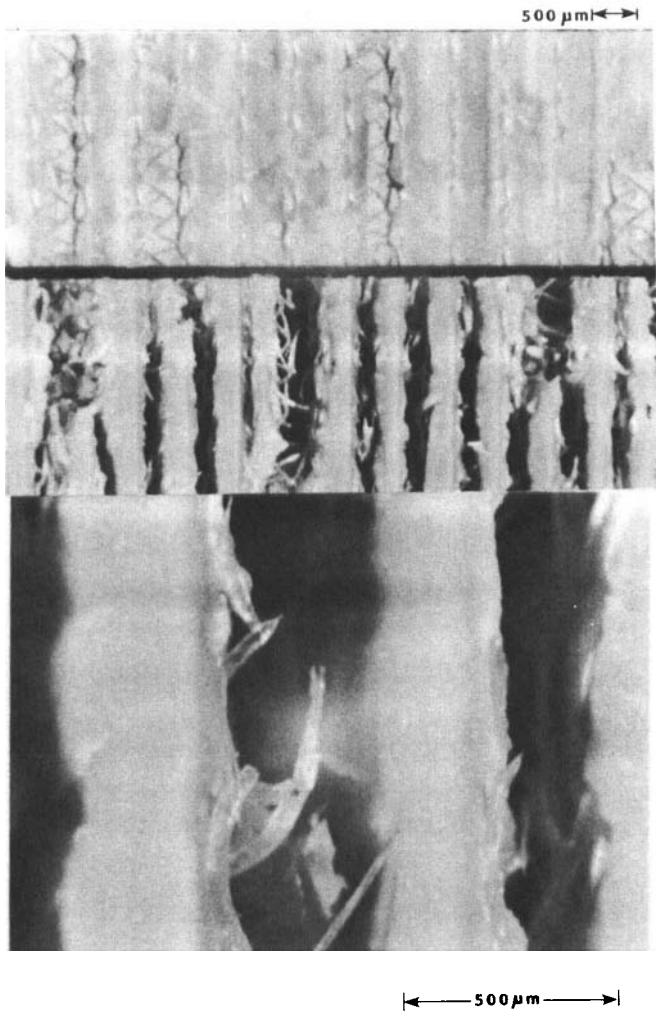

FIGURE 18 Fracture surfaces of a stiff-adherend specimen tested under pinned boundary conditions.

strain to failure differed by less than 3% and did not appear to be affected by gripping condition.

The data can also be compared with existing data obtained from single lap shear and napkin-ring tests. The manufacturer's listed value of lap shear strength is 35.5 MPa which falls between the strengths discussed above. The implication is that the pinned gripping condition gave rise to a purer state of shear and thus a higher strength. Stringer[22] used a napkin ring specimen to compare the stress-strain behavior of a number of structural adhesives. Among the compared adhesives was a supported, rubber-modified epoxy (adhesive D,[22]). The shape of the stress-strain curve of the adhesive was quite similar to that of Figure 17, the stress-strain behavior of the adhesive in the pinned specimens. The shear

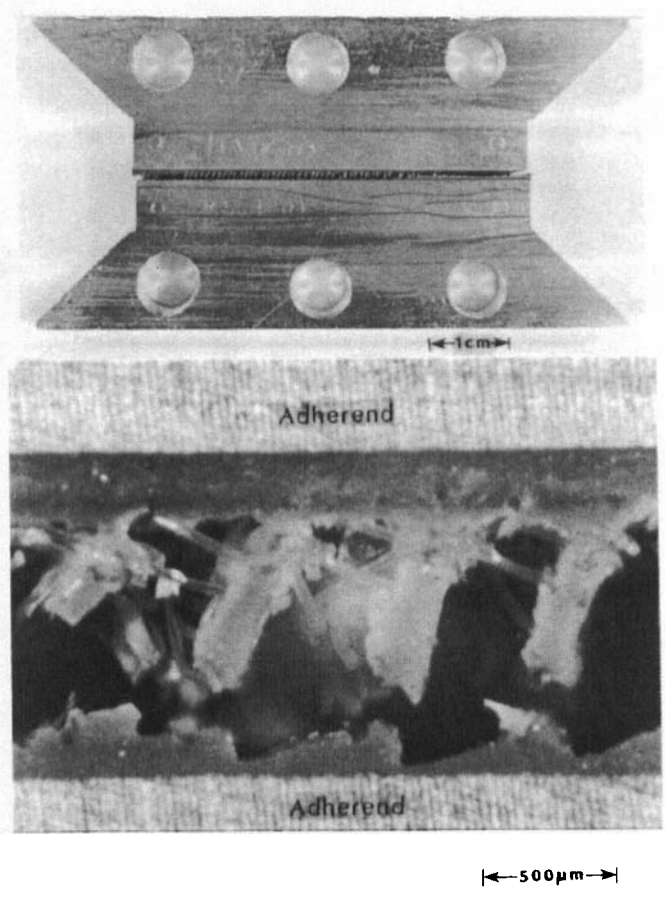

FIGURE 19 Profile of fracture surfaces of a stiff-adherend specimen tested under pinned boundary conditions.

modulus, strength and strain to failure of adhesive D were 722 ± 203 MPa, 46.3 MPa and 51%, respectively. The ultimate strength and strain were thus quite similar, although the FM 300 modulus derived here is about 50% lower.

An interesting comparison of the data can also be made with data obtained from neat films of FM 300 that were subjected to uniaxial tension.[23] The tensile modulus, ultimate strength and strain to failure were 2.285 GPa, 48.5 MPa, and 3.8% respectively. The Poisson's ratio was 0.4, leading to a shear modulus of 815.9 MPa which is more than twice the shear modulus of the adhesive determined *in-situ* here. The neat film strength in tension was a bit higher than the *in-situ* shear strength, but there was a large difference in strains to failure, proably because more damage can be sustained for the *in-situ* case. In that case, an initial microcrack arrested by the adherends and other microcracks are forced to grow, whereas in tensile thin film tests one microcrack can result in final failure of the specimen.

It is possible that the scrim cloth contributed to the difference between the shear modulus that was obtained from the stiff adherend specimen and the value that was derived from the neat tensile coupons through the relationship for isotropic materials between shear modulus, tensile modulus and Poisson's ratio:

$$G = \frac{E}{2(1+\upsilon)}. \tag{3}$$

The woven scrim fibers will tend to make the adhesive layer behave more like an orthotropic material, depending on how thin the overall adhesive layer is. Under such conditions the use of (3) is incorrect and the finite element analyses would also have to be suitably modified. A further consideration is that the neat tensile coupons were obtained from four layers of adhesive tape (and therefore scrim cloth), whereas the stiff adherend specimens contained only one. Depending on how the scrim layers meshed in the tensile coupons, there is the possibility of further reinforcement there that might give rise to a higher tensile modulus and thus a higher derived shear modulus.

CONCLUSIONS

Stress analyses of three main classes of specimens that might be used for *in-situ* testing of structural adhesives were conducted. The purpose of the stress analysis was to determine the purity and uniformity of the stress states under shear, bond-normal and thermal loadings. The main classes of specimens under consideration where the napkin-ring, cone-and-plate, and stiff-adherend specimens. Within each class, various edge modifications to the basic adherend geometry were made in order to improve the uniformity of the stress state. Of the specimen geometries examined, the cone-and-plate geometry was the least promising in terms of stress uniformity. The main differentiation between the napkin-ring and stiff-adherend geometry arose in the residual stress state with the latter specimen providing the most uniform state. Within the stiff adherend family of specimens the geometry having a straight notch with rounded adherends (SNRA) was the optimum choice, providing reasonable uniformity without stress concentrations for all load cases.

Procedures were developed for fabrication and testing of the stiff-adherend SNRA specimen. The butterfly-shaped specimens require more fabrication steps than many other specimens. However, batches of specimens having the same surface preparations and cure history can be made by bonding together adherend blocks having the butterfly shape and the slicing out specimens of appropriate thickness from the cured block. Grip and specimen alignment is critical and should be carefully maintained. The way in which the load was transferred into the specimen from the grips had a strong effect on the adhesive strengths that were realized. Pin joining the adherends to the grips was found to be more effective than clamping the adherends with the grips and resulted in a shear strength that was 27% higher than manufacturers' quoted values obtained from

lap shear tests. The different shear strengths were reflected in markedly different fracture surfaces. The higher shear strengths were associated with very rough, ridged fracture surfaces that resulted from tensile microcracks oriented at 45° to the bond line (indicating pure shear) that extended across the bond line before linking to cause final failure. The fracture surfaces associated with the lower strengths were much smoother, indicating the presence of normal stress components. The two methods of load transfer into the specimen did not affect the determination of shear modulus which was however consistently 50% of the values determined from tensile tests of neat adhesive films of FM 300. The shear modulus was also 50% of that of a generically similar adhesive. The strain to failure was not affected by load transfer method and was more than a factor of 10 greater than neat adhesive film tensile values.

Acknowledgments

This work was supported under the DARPA/ONR High Temperature Adhesives Program through a subcontract from Hughes Aircraft Company; the support is gratefully acknowledged. Many thanks are also due to Jeanie Paterson who prepared the manuscript.

References

1. O. Voklersen, *Luftfahrtforschung* **15,** 41 (1938).
2. M. Goland and E. Reissner, *J. Appl. Mechanics,* Series E of the Transactions of the ASME **66,** A17 (1944).
3. V. L. Hein, and F. Erdogan, *Intern. J. Fracture Mechanics* **7,** 317 (1971).
4. J. A. Harris, and R. D. Adams, *Int. J. Adhesion and Adhesives* **4,** 65 (1984).
5. R. D. Adams and W. C. Wake, in *Structural Adhesive Joints in Engineering* (Elsevier Applied Science Publishers, New York, 1984), p. 27.
6. T. B. Frazier, in *Proceedings of National SAMPE Technical Conference,* **Vol. 2** (Aerospace Adhesive and Elastomers, Dallas), (1970), p. 71.
7. T. R. Guess, R. E. Allred F. P. Gerstle Jr., *J. Testing and Evaluation,* JTEVA **5,** 84 (1977).
8. V. Weissberg and M. Arcan, "A uniform pure shear testing specimen for adhesive characterization," *Proc. Int. Symp. on Adhesive Joints: Testing, Analysis and Design,* ASTM STP981, **28** (1988).
9. N. Goldenberg, M. Arcan and E. Nicolau, *ASTM STP*247, 115 (1958).
10. M. Arcan, Z. Hashin and A. Voloshin, *Experimental Mechanics* **18,** 141 (1978).
11. W. T. McCarvill and J. P. Bell, *J. Adhesion* **6,** 185 (1974).
12. J. W. Grant and J. N. Cooper, *ibid.* **21,** 155 (1987).
13. J. W. Grant, in *Adhesion Science Review* **1,** 187 (1987) H. F. Binson, J. P. Wightman and T. C. Ward, Eds.
14. K. M. Liechti, T. Freda and T. Hayashi T., "Determining the constitutive and fracture properties of structural adhesives," in *Adhesion Science Review* **1,** 199 (1987), H. F. Brinson, J. P. Wightman and T. C. Ward Eds.
15. M. L. Williams, *J. Appl. Mechanics* **19,** 526 (1952).
16. E. H. Dill, A. L. Deak and W. F. Schmidt, *Handbook for Engineering Structural Analysis of Solid Propellants,* CPIA Publication 214, (1971), Chapter 5.
17. E. B. Becker, *et al.,* "Viscoelastic Stress Analysis of Adhesively Bonded Joints Including Moisture Diffusion," AFWAL-TR-84-4057, 1984.
18. E. B. Becker and T. H. Miller, "TEXPAC-NL: A Finite Element Code for Elastomeric Analysis," *Users Manual,* 1987.
19. G. H. Lindsey, R. A. Schapery, M. L. Williams and A. R. Zak, "The Triaxial Tension Failure of Viscoelastic Materials," Aerospace Research Laboratories Report, ARL 63–152 (1963).

20. T. Hayashi, "Pure Shear Testing of Adhesives *In-Situ*," M.S. Thesis University of Texas at Austin, Engineering Mechanics Research Laboratory, EMRL Report #87/7 (1987).
21. R. D. Adams, J. Coppendale and N. A. Peppiatt, *J. Strain Analysis* **13,** 1 (1978).
22. L. G. Stringer, *J. Adhesion* **18,** 185 (1985).
23. K. M. Liechti and T. Freda, "On the use of laminated beam specimens for the determination of pure and mixed-mode fracture properties of structural adhesives," *J. Adhesion,* in press.